

# $gg \rightarrow \gamma f \bar{f}$ in the strongly interacting phase of the MSSM

D. A. Demir<sup>1</sup>

*Middle East Technical University, Department of Physics, 06531, Ankara, Turkey*

## Abstract

$gg \rightarrow \gamma f \bar{f}$  scattering is discussed in the strongly interacting phase of the MSSM. The rate for the decay  $h \rightarrow \gamma f \bar{f}$  is computed in the MSSM and SM, and values of the Higgs–sfermion coupling needed for the former to dominate on the latter are identified. It is found that the MSSM signal dominates on the SM one for Higgs–sfermion couplings well below the one needed for developing stopponium bound states via Higgs mediation.

---

<sup>1</sup>Present Address: High Energy Section, ICTP, Trieste, Italy

The Minimal Supersymmetric Model contains a total of five Higgs scalars; two charged, two CP-even and a CP-odd one. It is known that for most of the parameter space allowed by the present experimental data [1], the MSSM is in the decoupling regime [2] in which one of the CP-even scalars, CP-odd scalar and charged scalar are rather heavy and almost degenerate in mass, while the mass of the lightest CP-even scalar,  $h$ , assumes its upper bound,  $m_h \lesssim 95 - 130$  GeV [3], depending on the region of the parameter space. In the decoupling regime the lightest Higgs,  $h$ , has almost the same properties as the SM Higgs boson, and presently its mass is bounded from below by  $m_h \gtrsim 90$  GeV [1] by the negative Higgs search at LEP2. With this mass bounds,  $h$  will be the only Higgs scalar accessible at the LHC [4].

After the ending of LEP2 era, search for the Higgs particle will continue at the LHC [4]. At the LHC energies the Higgs particle is expected to be produced via gluon-gluon fusion  $pp \rightarrow gg \rightarrow h$  [5]. The produced Higgs particle subsequently decays either to  $\gamma\gamma$  for  $M_Z \lesssim m_h \lesssim 130$  GeV or ( $ZZ \rightarrow 2\ell^+2\ell^-$ ) for  $130\text{GeV} \lesssim m_h \lesssim 155\text{GeV}$  [6, 7], or ( $W^+W^- \rightarrow \ell^+\nu\ell'^-\bar{\nu}$ ) for  $155\text{GeV} \lesssim m_h \lesssim 2M_Z$  [8]. With the huge irreducible  $\gamma\gamma$  background, isolation of the narrow  $\gamma\gamma$  resonance [7, 9] requires the design of high-resolution detectors [7]. Besides these rare decays of the Higgs particle, the diHiggs production process  $gg \rightarrow \phi_1\phi_2$  is also crucial for constructing the Higgs sector of the model under concern as the trilinear Higgs couplings can be probed directly with such two scalar final states [10].

Single isolated photon production at LHC dominated by the tree-level transition  $gq \rightarrow \gamma q$ , will be an important test of the QCD at large  $p_t^\gamma$  [11]. Moreover,  $h \rightarrow \bar{f}f$  can be a possible signature of the intermediate mass Higgs boson if there is a high  $p_t$  jet accompanying the produced Higgs [12]. Thus, in addition to the two-body decays of the produced Higgs, it seems necessary to have a discussion of the three-body decay process  $gg \rightarrow \gamma\bar{f}f$  whose signature consists of a single isolated  $\gamma$  and a pair of light fermions to which the produced  $h$  decays.

Although the processes mentioned above are highly important for discovering the Higgs particle at the LHC, there remains still the question of which model this would-be discovered scalar particle belongs to. To find at least an indirect evidence for the underlying model, one has to exploit those properties of the model not shared by the other candidate ones. Following the

detailed discussion in [2], one immediately observes that, in the decoupling regime, the SM and MSSM differs from each other mainly by the existence of the supersymmetric partners of the known SM particles in the MSSM particle spectrum. Therefore, in the decoupling regime one can obtain, albeit indirect, some manifestations of the low-energy supersymmetry. In this sense, that region of the MSSM parameter space in which the supersymmetric partners of the known fermions couple to the Higgs particle strongly may provide a room for obtaining some signal of the supersymmetry. Indeed, as recently proposed, when the stop trilinear coupling becomes large, one faces with new phenomena ranging from the sfermion bound states to charge and/or color breaking minima [13]. This very portion of the entire MSSM parameter space can cause certain collision processes to have amplified rates which, if observed, can be taken as an indication for the MSSM to be the underlying model. In fact, recently LHC- approved processes  $h \rightarrow \gamma\gamma$  and  $h \rightarrow gg$  have been analyzed in this kind of parameter space [14].

In this letter we discuss the process  $gg \rightarrow h^* \rightarrow \gamma(Z^*, \gamma^*) \bar{f}f$  in that region of the MSSM parameter space in which

- the heavy Higgs scalars are much heavier than the  $Z$  boson, and  $|\alpha| \approx |\beta - \pi/2|$  up to corrections  $\mathcal{O}(M_Z^2/M_A^2)$  [2], and
- the lightest Higgs  $h$  couples to the light stop with a strength as large as the one needed for developing light stop bound states via Higgs mediation [13].

As in  $gg \rightarrow \gamma\gamma$  there is a non-negligible background represented mainly by the box diagrams. However, if the final state fermions are tagged properly together with the detection of the photonic jet it may be easier to observe this event if it has sufficiently large branching fraction [11, 12]. Therefore, below we compare the predictions of the MSSM and the SM in analyzing the process under concern.

In computing one-loop  $h\gamma V^*$  ( $V = \gamma, Z$ ) vertex  $h\tilde{t}_1\tilde{t}_1$  ( $\tilde{t}_1$  being the light mass-eigenstate stop) coupling will be denoted by  $g_{h\tilde{t}}$ . When expressed in terms of the basic parameters of the MSSM Lagrangian  $g_{h\tilde{t}}$  is seen to contain two parts: The D-term contributions (proportional to the SU(2) coupling  $g$ ), and F-term and soft breaking contribution (proportional to top Yukawa coupling and related to the stop left-right mixing mass parameters). In this

sense, large  $g_{h\tilde{t}}$  implies automatically large stop left-right mixing so that the stop mixing angle becomes maximal  $\theta_{\tilde{t}} \approx \pi/4$ . The expressions for the stop masses, mixings, and  $g_{h\tilde{t}}$  can be found, for example, in [6, 15]. For convenience we will follow the notation of Weiler and Yuan in [6]. Moreover we introduce the 'fine structure' constant

$$\alpha_{\tilde{t}} = \frac{1}{16\pi} \frac{g_{h\tilde{t}}^2}{m_{\tilde{t}_1}^2} \quad (1)$$

where  $m_{\tilde{t}_1}$  stands for the mass of the light stop. This particular form for  $\alpha_{\tilde{t}}$  is chosen to suggest the formation of stopponium states via light Higgs mediation. As the explicit computations in [13, 16] show such bound states occur when  $\alpha_{\tilde{t}} \gtrsim 1.7(m_h/m_{\tilde{t}_1})$ . Here the main concern is not on the analysis of such bound states but the critical value of  $\alpha_{\tilde{t}}$  for which the MSSM prediction for the process under concern exceeds that of the SM by a given amount.

The basic Higgs search strategy at the LHC is the observation of gluon-gluon fusion to Higgs whose resonance shape, width and subsequent dominant decay mode are of central importance. As mentioned at the beginning, the  $\gamma\gamma$  decay mode is hard to detect, and thus, one generally searches for other decay signatures whose observation could be easier. In this context one recalls the recent works [17] which deal with the associated production of squarks with  $h$ . Discussion of the process  $gg \rightarrow \gamma \bar{f} f$  comprises gluon-gluon fusion to Higgs (requiring  $\Gamma(h \rightarrow gg)$ ) followed by the Higgs decay to  $\gamma \bar{f} f$  final state. Unless Higgs comes to its mass-shell the process loses its importance for the LHC Higgs search. The expression for  $\Gamma(h \rightarrow gg)$  can be found in [6, 15, 14]. On the other hand the rate for  $h \rightarrow \gamma \bar{f} f$  reads as

$$R \equiv \frac{\Gamma(\text{MSSM}|h \rightarrow \gamma \bar{f} f)}{\Gamma(\text{SM}|h \rightarrow \gamma \bar{f} f)} = \frac{\int_{4m_f^2}^{m_h^2} ds A_{\text{MSSM}}(s)}{\int_{4m_f^2}^{m_{h_0}^2} ds A_{\text{SM}}(s)} \quad (2)$$

in units of the SM rate with  $m_f$  being the mass of the produced fermion and  $\sqrt{s}$  is the invariant mass flow to  $\bar{f}f$  channel. Here  $m_h$  ( $m_{h_0}$ ) is the mass of the lightest Higgs in the MSSM (Higgs mass in the SM), and they are taken equal in writing  $R$ . The MSSM integrand  $A_{\text{MSSM}}(s)$  is given by

$$\begin{aligned} A_{\text{MSSM}}(s) = & \left(1 - \frac{s}{m_h^2}\right)^3 \left(1 - \frac{4m_f^2}{s}\right)^{1/2} \left\{ \frac{2}{3} (s - m_f^2) \left[ \frac{|A_\gamma(s)|^2}{s^2} \right. \right. \\ & \left. \left. + 2v_f \frac{\text{Re}[A_\gamma(s)A_Z(s)]}{s(s - M_Z^2)} + (a_f^2 + v_f^2) \frac{|A_Z(s)|^2}{(s - M_Z^2)^2} \right] \right\} \end{aligned} \quad (3)$$

$$- a_f^2 m_f^2 \frac{|A_Z(s)|^2}{(s - M_Z^2)^2} \}$$

where  $v_f = (I_3^f - 2Q_f s_W^2)/(s_W c_W)$  and  $a_f = -I_3^f/(s_W c_W)$  are the vector and axial-vector couplings of the  $Z$  boson, and  $A_\gamma$  and  $A_Z$  are the loop functions describing  $h\gamma\gamma^*$  and  $h\gamma Z^*$  effective vertices, respectively. These vertex formfactors get contributions from all the charged particle of the model under concern (SM or MSSM). In the MSSM, one has

$$A_{\gamma,Z} = A_{\gamma,Z}^{W^\pm} + A_{\gamma,Z}^{f^\pm} + A_{\gamma,Z}^{\chi^\pm} + A_{\gamma,Z}^{H^\pm} + A_{\gamma,Z}^{\tilde{f}^\pm} \quad (4)$$

representing, respectively, the loops of  $W$ -boson, charged fermions, charginos, charged Higgs boson, and charged sfermions.  $A_{\text{SM}}$  in (2) can be obtained from (3) by keeping only  $W$ -boson and charged fermion contributions in (4). The explicit expressions for the loop functions  $A_{\gamma,Z}^{i^\pm}$  can be found in [6]. As described there, there are three independent loop functions determining  $A_{\gamma,Z}^{i^\pm}$ :  $I[m_{loop}^2, m_h^2, s]$ ,  $J[m_{loop}^2, m_h^2, s]$  and  $K[m_{loop}^2, m_h^2, s]$  which have the respective limiting values  $1/2$ ,  $1/24$  and  $1/6$  when  $m_{loop}^2 \gg m_h^2, s$ . Hence  $A_{\gamma,Z}^{i^\pm}$  remain non-vanishing even for infinitely heavy loop masses  $m_{loop}$ . The  $W$  boson contribution, for example, is sensitive to  $I$  and generally dominates over other contributions. In this sense one expects the SM contribution to be large compared to the SUSY contributions. This conclusion holds also when both gauge bosons are on their mass shell [6, 15].

Therefore, it is convenient to search for an appropriate region of the supersymmetric parameter space where  $h \rightarrow \gamma\gamma$ ,  $h \rightarrow gg$ , and  $h \rightarrow \gamma\bar{f}f$  can be enhanced due to supersymmetric contributions [6, 15]. The first two process have been discussed in [14] as a function of relatively large Higgs-sfermion couplings. Here we are mainly concerned with  $h \rightarrow \gamma\bar{f}f$  in the strongly interacting phase of the MSSM where  $\alpha_{\tilde{t}}$  is large. The  $W$  boson and fermion contributions are common to both SM and MSSM. We include only sfermions into the discussion as the others (charginos and charged Higgs) give small contributions in the parameter space employed here. Among the sfermions the most important contributions follow from scalar top quarks as they can be relatively light due to large top Yukawa coupling. Thus, to a good approximation, we represent the supersymmetric contributions by  $W$ , fermion and light stop loops the latter being the pure supersymmetric contribution compared to the SM.

The contribution of the light stop loop has the form

$$A_{\gamma,Z}^{\tilde{t}^\pm} \propto \frac{2M_W}{m_{\tilde{t}_1}} \sqrt{\frac{\alpha_{\tilde{t}}}{\alpha_W}} J[m_{\tilde{t}_1}^2, m_h^2, s] \quad (5)$$

where  $\alpha_W = g^2/(4\pi)$ . To see the consistency of the light stop dominance, one recalls that large stop left–right mixings make  $\alpha_{\tilde{t}}$  large and  $\tilde{t}_1$  light simultaneously. This causes  $A_{\gamma,Z}^{\tilde{t}^\pm}$  to dominate over other loop contributions, and enhance  $R$  significantly. In this sense sfermion contributions, here light stop, can cause spectacular enhancement in  $R$  whereby making supersymmetric contributions observable.

Fig. 1 shows the variation of  $R$  with  $\alpha_{\tilde{t}}$  for a light  $\tilde{t}_1$ ;  $m_{\tilde{t}_1} = M_Z$ . Here solid and dashed curves correspond to  $m_h = M_Z$  and  $m_h = 2M_Z$ , respectively. For the given value of  $m_{\tilde{t}_1}$ ,  $\alpha_{\tilde{t}} = 0.2$  ( $\alpha_{\tilde{t}} = 1.7$ ) corresponds to  $g_{h\tilde{t}} \sim 300$  GeV ( $g_{h\tilde{t}} \sim 900$  GeV). In this and the next figure we assume a relatively large  $\tan\beta$ , that is,  $\alpha \sim 0$ . As is seen from the figure,  $R$  increases monotonically with  $\alpha_{\tilde{t}}$  due to the fact that the stop contribution to  $R$  increases, as suggested by the formula (5). However, when the Higgs mass is doubled increase of  $R$  is automatically slowed down (dashed curve). Thus, it is more likely to observe the contribution of the stops for a light enough stop and Higgs. Besides these, one notices that, in general,  $R$  is well above unity so that in both cases, despite the uncertainties in various parameters, it may be quite easy to observe the excess in  $R$ . Since the stop contribution is able to dominate over the W–boson contribution, it is quite large compared to the fermion contributions, so that one expects  $hgg$  vertex be dominated by stops as well. The upper limit on  $\alpha_{\tilde{t}}$  is chosen to be  $\sim 1.75$  which is the threshold value for developing the color–singlet stop bound states via Higgs mediation [16]. Thus, stop contribution is able to dominate over those of W and fermions before the onset of the bound state formation. Once the light stop bound state is formed the subsequent evolution of the system (depending on its lifetime) could be quite different. Introduction of such bound states to the particle spectrum can even replace the properties of the Higgs particles [13] falsifying the Higgs search strategy at the colliders, in particular, at the LHC.

Figure 2 shows the same quantities in Fig. 1 for a heavier stop  $m_{\tilde{t}_1} = 2M_Z$ . It is seen that both curves are rescaled according to Fig. 1, that is, now the enhancement in the quantities is much smaller. The given range of  $\alpha_{\tilde{t}}$  again corresponds to the same range for  $g_{h\tilde{t}}$  mentioned in the previous

paragraph. Since,  $\alpha_{\tilde{t}}$  is below  $\sim 0.8$  there is no chance for bound state formation.

Given the uncertainties in the Higgs masses and huge  $\gamma\gamma$  background it is an issue of precision for LHC detectors to observe the Higgs signal. For this and similar technical reasons one has to consider new mechanisms allowing an easier way of detection. In this sense, the final state discussed here constitutes a possible way of obtaining an enhanced single photon signal. Observation of the charged particles is not a problem for the experiment, and with the given direction and invariant mass of the  $\bar{f}f$  pair it might be easier to detect the single prompt photon [11].

For the process under concern, the interesting thing occurs for larger values of  $\alpha_{\tilde{t}}$  for which the threshold value for developing stop bound states is exceeded. Once the stops develop bound states they may easily interfere with the Higgs boson signal sought. As was already discussed in [13] the stop bound states may develop non-zero vacuum expectation values whereby behaving as some component to the Higgs boson signal. In such cases even the existing bounds on the Higgs boson does not hold and new phenomenological issues arise. In this analysis we have avoided entering this realm of the couplings; however, despite this MSSM signal may dominate over the SM signal in a wide range of the fine structure constant  $\alpha_{\tilde{t}}$ .

Author thanks to G.Belanger, F.Boudjema, and K.Sridhar for their helpful remarks.

## References

- [1] Particle Data Group Homepage: <http://pdg.lbl.gov/>.
- [2] H. E. Haber, CERN-TH/95-109, hep-ph/9505240.
- [3] M. Carena, M. Quiros, C. E. M. Wagner, Nucl. Phys. **B461** (1996) 407; H. E. Haber, R. Hempfling, A. Hoang, Z. Phys. **C75** (1997) 539; J. R. Espinosa, M. Quiros, Phys. Rev. Lett. **81** (1998) 516.
- [4] J. F. Gunion, A. Stange, S. Willenbrock, hep-ph/9602238; N. V. Krasnikov, V. A. Matveev, Phys. Part. Nucl. **28** (1997) 441.
- [5] H. Georgi, S. Glashow, M. Machacek, D. Nanopoulos, Phys. Rev. Lett. **40** (1978) 692.

- [6] T. J. Weiler, T.-C. Yuan, Nucl. Phys. **B318** (1989) 337; T. G. Rizzo, Phys. Rev. **D22** (1980) 178.
- [7] CMS Collaboration, Report CERN-LHCC 94-38; ATLAS Collaboration, Report CERN-LHCC 94-43.
- [8] M. Dittmar, H. Dreiner, Phys. Rev. **D55** (1997) 167.
- [9] D. P. Roy, hep-ph/9803421; C. Kao, hep-ph/9802343; J. A. Bagger, hep-ph/9709335; Z. Kunszt, hep-ph/9704263.
- [10] S. Dawson, S. Dittmaier, M. Spira, hep-ph/9805244; T. Plehm, M. Spira, P. M. Zerwas, Nucl. Phys. **479** (1996) 46; M. Spira, A. Djouadi, D. Graudenz, P. M. Zerwas, Nucl. Phys. **B453** (1995) 17; E. W. N. Glover, J. J. van der Bij, Nucl. Phys. **B309** (1988) 282.
- [11] P. Aurenche, R. Baier, M. Fontannaz, D. Schiff, Nucl. Phys. **B297** (1988) 661.
- [12] R. K. Ellis, I. Hinchliffe, M. Soldate, J. J. van der Bij, Nucl. Phys. **B297** (1988) 297.
- [13] A. Kusenko, V. Kuzmin, I. I. Tkachev, Phys.Lett. **B432** (1998) 361; G. F. Giudice, A. Kusenko, Phys. Lett. **B439** (1998) 55.
- [14] A. Djouadi, Phys. Lett. **B435** (1998) 101.
- [15] J. F. Gunion, H. E. Haber, G. Kane, S. Dawson, *The Higgs Hunter's Guide*, Addison-Wesley, New York, (1990).
- [16] L. D. Leo, J. W. Darewich, Can. J. Phys. **70** (1992) 412.
- [17] A. Djouadi, J.-L. Kneur, G. Moultaka, hep-ph/9903218; Phys. Rev.Lett. **80** (1998) 1830.



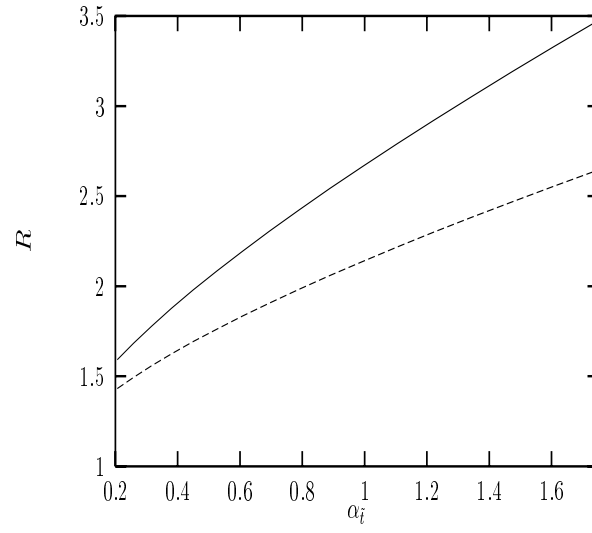


Figure 1: Variation of the ratio  $R$  in (2) with  $\alpha_{\tilde{t}}$  for  $m_{\tilde{t}_1} = M_Z$ ,  $m_h = M_Z$  (solid curve) and  $m_h = 2 M_Z$  (dashed curve).  $\bar{b}b$  final states are assumed.

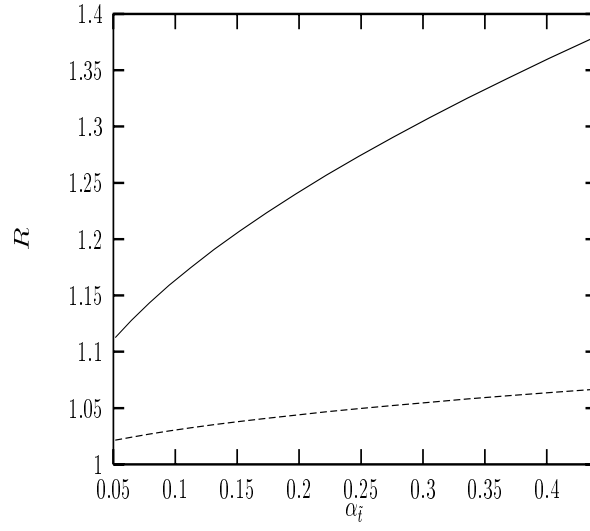


Figure 2: Variation of the ratio  $R$  in (2) with  $\alpha_{\tilde{t}}$  for  $m_{\tilde{t}_1} = 2 M_Z$ ,  $m_h = M_Z$  (solid curve) and  $m_h = 2 M_Z$  (dashed curve).  $\bar{b}b$  final states are assumed.